# An Improved Technique for VCG Signal Compression using VMD and TQWT

H. Gupta[1], Aditya Tiwari[1*], A. Kumar[1],

[1]PDPM-Indian Institute of Information Technology Design and Manufacturing, Jabalpur, 482005, M.P., India

**E-mail:** himanshu.gupta.signal@gmail.com, adityatanu7@gmail.com, anilkdee@gmail.com

***Abstract***

***Purpose***: Medical practitioners specially cardiologist utilize their expertise to assess the diagnosis of heart's electrical activity in human body. Hence, in order to accurately represent these vital signals, a physiological monitoring technique known as vector-cardiography (VCG) is used. This work focuses on denoising the VCG signal during the acquisition process as well as compressing the signal for subsequent storage. Here, the modeled noise is powerline noise.

***Methods:*** The proposed method uses variational mode decomposition (VMD) & notch filter, and facilitates the utilization of empirical mode decomposition (EMD), tunable Q-factor wavelet transform (TQWT) techniques for compression. Here, compression is achieved by using different mode functions of the denoised signals by employing TQWT, quantization and run-length encoding.

***Results:*** To evaluate the performance, various metrics such as mean-square-error, peak-signal-to-noise-ratio, percent-root-difference, compression-ratio, and signal-to-noise-ratio have been employed for both denoising and compression purposes. The denoising performance at $SNR_{INPUT}$ of 10dB, shows an *MSE* of $1.11*10^{-4}$, a *PSNR* of 40.85, $SNR_{OUT}$ of 26.61, a $SNR_{IMP}$ of 16.61, at a *PRD* of 5.12 respectively. The compression performance of the proposed method highlights a *CR* of 71.38 at a *PRD* of 4.44, a *PSNR* of 10.41, along with an *SNR* of 19.96, with a *QS* of 16.05, and obtaining a *MSE* of $2.00*10^{-4}$.

***Conclusion:*** The proposed method successfully removes the powerline noise in the signal. The observations and results obtained from these metrics reinforce the effectiveness of the proposed method as a denoising and compression technique to set a precedent for future work in the field of VCG signals.

***Keywords*—Dead-zone quantization, Decomposition methods, Notch filter, Run-length encoding, Tunable Q-factor wavelet transform, Vectorcardiography.**

## 1 Introduction

The human body comprises of various metabolic activities governed by its own set of principles. These principles adhere to natural laws and generate specific rhythmic activities [1], which can be translated into physical form through the visualization of data. The use of these data not only helps in gaining additional information about the patterns associated with them but also provides encoded information related to other bodily functions. These signals can be recorded or visualized via special machines leading to development of techniques with different modalities such as electrocardiography (ECG) [2], electroencephalography (EEG) [3], vectorcardiography (VCG) [4], etc. For instance, to measure the electrical activities of the heart, ECG or VCG can be considered as viable options. These signals are measured after capturing via application of leads, that are placed on specific body parts [5]. In ECG, the number of leads increases the quality of information recorded from the body. But in case of VCG, 3 leads are sufficient to properly capture overall functioning of the heart, while providing additional scope of observation in form of magnitude and direction from the electrical vectors. The signals thus obtained require further processing to facilitate improvements in data quality. Additionally, various state-of-the-art techniques have been proposed that incorporate these signals, broadening the scope of research opportunities in different fields, such as; denoising [6], security [7], disease detection, classification [8,9], monitoring [10], compression [11], and telemedicine [12].

An acquired signal may contain disturbances during acquisition, transmission, or storage operations. These disturbances can corrupt the data, leading to undesired results. In order to remove these "noise" components from the signals, specialized

denoising algorithms have to be employed. In case of ECG or VCG, channel noise [13], base-line wander [14], power-line-interference (PLI) [15], muscle artefacts [16], random noise, composite noise, and instrumentation noise determines the dominant factors affecting the quality of signals [17]. These unwanted components can be removed using different denoising methods broadly classified into decomposition based, machine learning based, wavelet based, bayesian filter based, and hybrid models. The decomposition based techniques include EMD (empirical mode decomposition) [18], and VMD (variational mode decomposition) [19]. In EMD, the empirically determined data-driven algorithm provides considerable space for adaptability in accordance with the signal without involving any basis functions. Whereas, in VMD the limitation of mode aliasing present in the EMD is mitigated by VMD involving a constraint problem, the solution to which gives the mode functions. The deterministic nature of the algorithm provides a stable, robust mechanism for its application to various filtering scenarios. On the other hand, the wavelet based denoising method, decomposes the signal into basis functions based on mother wavelet. As this method holds the ability to constrain the energy of signal into a smaller number of coefficients, it also becomes a suitable choice to be employed in denoising of the VCG signal. Other methods such as notch filter [19]; non-local means filter (NLM) [20], employs weighted averaging method for removing noise; mean/average filter (AF) that suppresses noise using the mean operation of segment of the signal; median filter (MF), utilizes a window, where central value is replaced with median value in the window. Moreover, some other filters that suppress noise levels includes adaptive filters, Bayesian filters, Kalman filters, extended Kalman filters, and various optimization methods [21]. The suppression of noise can also be performed by using machine learning techniques, like, CNN based methods, deep learning based autoencoders (DAE), and DNN. The essential characteristics of these algorithms should include the capability to enhance signal quality and also to retain information content during the subsequent denoising process.

Following the implementation of the noise removal process, the next step is the compression of the corresponding signal. In VCG telemonitoring, the continuous data generated are substantial enough to require dedicated storage options, making the use of compression algorithms essential for efficient storage [22]. In this work, the objective of compressing the signal is to enable reduction in storage space occupied by the signal. Here, the compression can be categorized broadly in three classes [23] namely the transformation domain (TD) based, direct data compression (DDC) based, and parametric extraction (PE) based methods. The TD based techniques include Wavelet transform [24], Fast Fourier transform [24], Discrete Cosine Transform [24], Karhunen Loeve transform (KLT) [11], Tunable Q-wavelet Transform (TQWT) [25], etc, where the signals are encoded using the linear orthogonal transformation. Despite their high compression efficiency, these methods are limited by their high complexity and lossy nature. On the other hand, DDC based methods employ different prediction methods based or interpolation techniques for compression. Turning point (TP) [26], delta encoding [23], are some of the DDC methods. While in PE, parameters such as extremes' amplitude location, zero crossing intervals, and gradient change are extracted for compressing and reconstruction purposes [23]. There also exist lossless or lossy compression methods that reduce the space by encoding the signals via run-length encoding [27], utilizing "run" for minimizing repeatability of data in a stretch, and Huffman/arithmetic coding schemes [28].

This work introduces a novel decomposition assisted noise suppressed VCG compression method, where PLI noise altered, signals are removed using VMD and notch filter is tuned to center frequency. The filtered signals are then employed with EMD and TQWT to decompose the EMD's modes into coefficient matrix which when quantized thresholded, and encoded, compresses the signal. In nutshell, scope of the algorithm is to achieve two objectives: (i) Denoise the signal. (ii) Compress the signal. Since, the proposed work is to analyze VCG signals, which has the same characteristics as that of ECG signals [29], and is a field of research rarely touched, this work paves the way forward by consolidating the findings of the algorithm. The major contributions presented in the work are as follows:

(i) A comprehensive technique is designed that includes a preprocessing step for denoising, and a subsequent algorithm for compressing the VCG signal.

(ii) High compression ratio is achieved using a combination of EMD, TQWT, dead-zone quantization, and RLE.

This article comprises of "Methodology" section; providing brief information on the dataset, preliminary concepts of various algorithms utilized in the development of this study, and detailed overview of the proposed method. The "Discourse" section discloses information about the visual and statistical observations obtained from analyzing the performance of proposed method. Finally, the "Conclusion" section concludes the findings and summarizes the objectives achieved in the work.

## 2 Methodology

### *2.1 Dataset*

To validate the performance of the proposed algorithm PTB diagnostic ECG database is utilized [30]. This dataset contains data of 549 subjects, which are digitized at a high resolution configuration at a sampling rate of 1000Hz. The 12 leads represents ECG in each record, whereas the last 3 leads contains VCG signals that were derived using the Frank lead system. In this study, VCG signals are considered for validation, where the data from 3 VCG leads represents information from the XYZ orthogonal planes serving as the planes of projection for these three components. The next sub section discusses all important preliminaries necessary for the development of this study.

### *2.2 Preliminaries*

The proposed method employs various methods with their respective underlying concepts, which have been discussed as per the literature mentioned below.

*(i) Notch filter*: A band-stop filter consisting of having a small stop band. Since PLI mostly exists in 50/60 Hz with a bandwidth of around less than 1Hz [15], narrow-band filters are necessary that removes specific tones and restricts alteration of other components of the spectrum. To resolve, these limitations, IIR (infinite impulse response) filters have been employed in this work which can be used as digital notch filters with the advantage of requiring lower filter order as compared to FIR (finite impulse response) filters for a given problem [31]. The frequency response of the notch filter utilized in the work is depicted in Fig. 1.

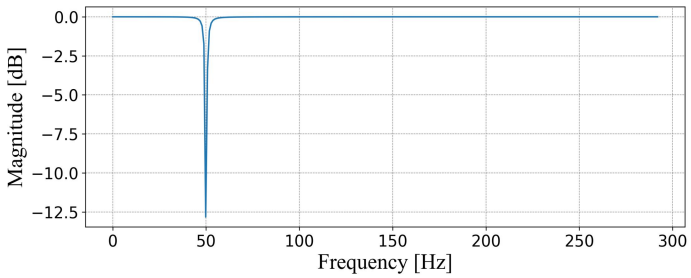


**Fig. 1.** Frequency response of notch filter with cutoff-frequency of 49.997 Hz.

*(ii) Variational mode decomposition (VMD):* The VMD decomposition method [32] deconstructs the signal into a number of IMFs (intrinsic mode functions) with its center frequency $\omega_K$ in the spectral domain, where the total number of IMFs, a signal can be decomposed is *K*. Here, the modes are considered to be AM-FM signal, where bandwidth of the signal is determined by the following procedure. In the first step, a unilateral frequency spectrum from an analytical signal is computed, followed by the usage of an exponential to shift the mode frequency to baseband. Finally, a constrained problem has been derived for the VMD algorithm. Afterwards, the reconstruction of the problem into an unconstrained problem is initiated, and the solution is estimated via minimization of the augmented Lagrangian function, as given in [32]. This process involves a parameter to balance the data-fidelity constraint, which is defined as $\mu$.

*(iii) Empirical mode decomposition (EMD):* The data-driven EMD process is a decomposition technique, where the IMFs are generated only if the following constraints are satisfied:

$$(a)\sum(\text{extremes})-\sum(\text{zero crossings})=0/1,$$

$$(b)\,\text{mean}\left(\text{envelope}_{\text{upper}},\text{envelope}_{\text{lower}}\right)\to 0.$$

The EMD algorithm utilizes the sifting process iteratively to produce IMF and a residue $r$ given by (1), where $d(K)$ represents the IMF, and the recombination of these variables yields the $x_{recomb}(n)$ signal.

$$x_{recomb}(n)=\sum_K d(k)+r. \tag{1}$$

*(iv) Tunable Q-wavelet transform (TQWT):* The TQWT algorithm [20,33] comprises of tunable parameters, namely the number of stages present in the transform $(S_t)$, oversampling rate $(R_{os})$, and Q-factor $(Q)$. Here, decomposition initializes with the deployment of iterative filter bank having two channels, with $m$ representing the total number of filter banks. Now, the signal spectrum is separated to form several high-pass and one low-pass sub-band signals at every decomposition level and respective sampling frequencies $(\gamma f_s, \varsigma f_s)$ associated with the sub-bands. The signals are generated using respective high-pass $f_h^m(\omega)$ and low-pass filters $f_1^m(\omega)$ with scaling parameters as $hps\,\gamma, lps\,\varsigma$ respectively. The process of decomposition and reconstruction of the signal is depicted in Fig. 2 with the utilization of high-pass $v_h(n)$ and low-pass $v_l(n)$ sub-band signals, where $x(n), y(n)$ represents the input and the reconstructed signal.


(a) (b)

**Fig. 2.** Block diagram representing a single level TQWT filter bank with: (a) analysis; and (b) synthesis filter bank.

*(v) Deadzone quantization (DZQ) method:* It utilizes a real valued variable, centered around zero and ranging from $[-th, th]$, where $th$ is the threshold value [34]. In order to have lower loss-compression ratio, selection of appropriate threshold value is important. As per mathematical formulation of DZQ discussed in [34], the $th$ is taken to be $(\max_{sb}-\min_{sb})/40$, where $\max_{sb}, \min_{sb}$ represents the maximum and minimum of the sub-bands. Now, a constraint has been applied for the selection of step size $(<2*th)$, where $step\,size = k*th$, and $k \in [1.20,\ 1.80]$ [34]. This whole process ensures quantization of the coefficients for further compressing the signals.

*(vi) Run-length encoding (RLE):* This lossless encoding technique, offers a simple method for reducing the data size of the signal while maximizing information retention. In this approach, the redundant sequences in the data are removed, where the detailed coefficients are repeated at a certain frequency [35].

### *2.3 Proposed method*

A novel VCG signal denoising and compression method is proposed to address the objectives identified in the literature. The whole process is summarized in the form of a flowchart depicted in Fig. 3. This section represents the working procedure and evaluation of the methods performance. The process begins with the loading of VCG data, that is subjected to PLI noise characteristics given by (2), where $x(n)$, $x_{noisy}(n)$ represents the input and noisy VCG signal, respectively:

$$x_{noisy}(n) = x(n) + PLI. \tag{2}$$

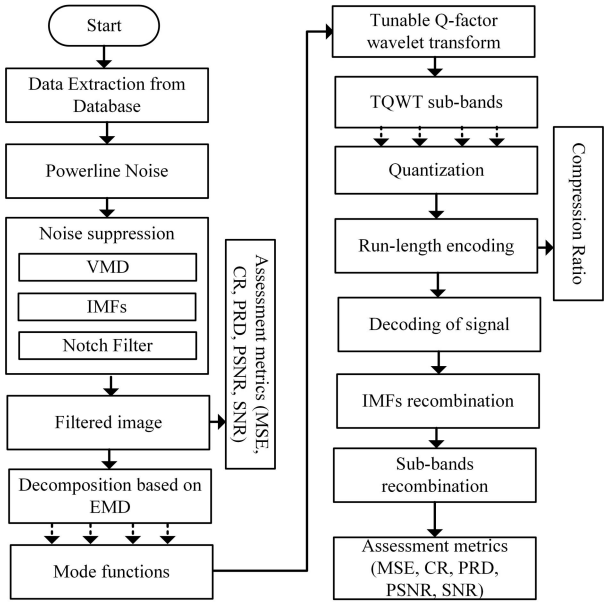


**Fig. 3.** The flowchart representing the method utilized in the proposed work.

The noise suppression is performed with the introduction of VMD that decomposes the signal into IMFs, and applying a manually tuned notch filter with sharp cut-off frequency. Here, the performance of VMD algorithm is dependent on the parametric inputs, namely $K$ and $\mu$, where the bandwise denoising of IMFs would be performed. Now, the notch filter suppresses the noise components present on each IMFs' spectrum, and is dependent on the quality factor, a parametric variable that characterizes the -3dB bandwidth of the notch filter in accordance with the center frequency; the normalized center frequency, obtained from the tuned center frequency and the sampling rate of the signal. These noise suppressed IMFs are now recombined to get the filtered signal $x_{filt}(n)$. Then, $x_{filt}(n)$ is utilized to estimate the performance of the pre-processing step through performance metrics such as *MSE, PSNR, SNR*$_{OUT}$, *SNR*$_{IMP}$, and *PRD* for specific input *SNR* values.

After the completion of the first objective, the second objective of compressing the signals would commence. In this process, for some defined *SNR*$_{IN}$, the $x_{filt}(n)$ is subjected to EMD process, to decompose the filtered signal into number of IMFs. These modes are then passed through the TQWT algorithm with their respective parametric values. The coefficient matrix obtained from the TQWT is now quantized, and thresholded using the DZQ method. The compression is finalized by applying RLE scheme to each of these TQWT sub-bands. To assess the performance of compression method, the metric, compression ratio is calculated using the encoded and the original coefficient matrices. Now, the retention of signal is achieved by decoding the RLE encoded coefficient matrix followed by the implementation of the inverse TQWT. The recombination of these extracted coefficient matrix in addition with reconstruction of the signal from the combination of EMDs' IMFs yields the final signal. Performance of the compression process introduced herewith is calculated with the utilization of *PRD, PSNR, SNR* and *MSE* metrics.

## 3 Discourse

The quantitative analysis for both denoising and compression process involves the following metrics: the input signal-to-noise-ratio $SNR_{IN}$, mean-square-error *(MSE)*, peak-signal-to-noise-ratio *(PSNR)*, output-signal-to-noise-ratio $(SNR_{OUT})$, percent-root-difference *(PRD)*, improved-signal-to-noise-ratio $(SNR_{IMP})$, compression ratio *(CR)*, and signal-to-noise-ratio *(SNR)*. Here, the algorithm's performance is divided into two parts with the estimation of metrics for; (i) denoising, and (ii) compression of the signals. Now, the denoising capability is calculated using $SNR_{IN}$ , $SNR_{OUT}$ , $SNR_{IMP}$ , *MSE, PSNR*, and *PRD* as represented by (2), (3), (4), (5), (6), (7), and (8) respectively:

$$SNR_{IN} = 10X\log_{10}\left(\frac{\sum_N |x(n)|^2}{\sum_N |x_{noisy}(n) - x(n)|^2}\right), \tag{3}$$

$$SNR_{OUT} = 10X\log_{10}\left(\frac{\sum_N |x(n)|^2}{\sum_N |x_{filt}(n) - x(n)|^2}\right), \tag{4}$$

$$SNR_{IMP} = SNR_{OUT} - SNR_{IN}, \tag{5}$$

$$MSE = \frac{\sum_N |x(n) - x_{filt}(n)|^2}{N}, \tag{6}$$

$$PSNR = 10X\log_{10}\left(\frac{(\max_{value})^2}{MSE}\right), \tag{7}$$

$$PRD = \sqrt{\frac{\sum_N |x(n) - x_{reconstructed}(n)|^2}{\sum_N |x(n)|^2}} X\,100\%, \tag{8}$$

where, $x(n), x_{noisy}(n), x_{filt}(n), x_{reconstructed}(n)$ represents the input, noise corrupted, filtered, and reconstructed signal for $N$ number of samples. For a given $SNR_{IN}$, better the $SNR_{OUT}$, it indicates lesser noise power contained in the signal. The improvement in *SNR* quality of the input signal with respect to output signal is measured by $SNR_{IMP}$. The metric *MSE* should have a lesser *MSE* score, defining the errors present in the corresponding signals. The *PRD* metric is indicative of the distortions existing in the signals with lower scores representing better quality signals. Lastly, the *PSNR* is used to evaluate the reconstruction quality in relation to the parent signal. The compression performance index includes $SNR_{IN}$, *CR*, *SNR*, *MSE, PSNR*, and *PRD* which are given in this section.

$$CR = \frac{size\,of\ x(n)\ in\,bytes}{size\,of\ x_{reconstructed}(n)\ in\,bytes}, \tag{9}$$

$$SNR = 10X\log_{10}\left(\frac{\sum_N |x(n) - \mu_{x(n)}|^2}{\sum_N |x_{reconstructed}(n) - x(n)|^2}\right). \tag{10}$$

Here, *CR* represents the compression achieved by the algorithm, and *SNR* can be described as the noise that resides after the reconstruction of the compressed signal. A high *SNR* score depicts a good reconstructed signal. The metrics discussed above provide the necessary framework to determine conclusive evidence, within an acceptable margin of error, for the proper functioning of the proposed method. The performance analysis of the developed approach is validated using PTB-DECG database having full 10 second signal i.e 10000 samples. As, the algorithm is initiated with the addition PLI noise, therefore the noise levels are considered in the performance estimation, and is calibrated using $SNR_{IN}$, such that $SNR_{IN} \in \{-10, -5, 0, +5, +10\}$ dB. For these $SNR_{IN}$, noise power are evaluated and added to the signal. Here, the noise is suppressed by first decomposing the signal into IMFs with the number varying in the range of 5 to 7, using VMD. The modes' number utilized in the work is 6. It is set such that the notch filter employed to suppress the PLI noise sustain maximum efficiency during the denoising process. Also, other parameters that enhances the decomposition performance is

$\mu(\in(150,200))$ and tolerance $(=10^{-5})$. The characteristics of the notch filter utilized here is controlled by the cutoff frequency, and the quality factor. Now, to obtain best results, manual tuning of the parameters has been performed to obtain cutoff frequency of 49.997 Hz, and quality factor of notch filter as 32.74. Moreover, the performance of denoising method is analyzed by the above-described assessment metrics and the estimated results from the method has been tabularized in Table 1, where it consolidates the performance of the technique on 5 different VCGs of the subjects. The graphical representation of each noisy VCG components are shown in Fig. 4 (b(i)-b(iii)). Also, the denoised signal obtained are depicted in c(i)-c(iii) of Fig. 4. Now, the filtered signal is then passed through a compression algorithm, where another decomposition method, EMD, is deployed to break the filtered signal into its constituent IMFs, with its number set to 5. Each of these IMFs is subsequently processed using the TQWT method, which further decomposes the IMFs into respective coefficient matrix. The parameters involved in the functioning of wavelet decomposition method includes $R_{OS}$, with an operational range of 3-10; Q-factor, takes values between 2 to 5; and decomposed levels set to 6. The intention is to compress the signal by reducing the size of these coefficient matrices. Afterwards, DZQ is applied with its parameter $K \in [1.20, 1.80]$ tuned manually, thresholding, and the RLE scheme to these coefficients achieves the second objective of this work i.e. compression.

Now, the compression ratio are calculated at this step followed by the recombination of all TQWT modes along with EMD's IMFs to get the final reconstructed signal. The performance is then estimated using the performance metrics, and is presented in Table 2. Also, the final reconstructed signal is illustrated in d(i)-d(iii) of Fig. 4. The e(i)-e(iii) of Fig. 4 represents how the final signal has been quantized (for 1sec duration), and clearly showcasing the effect of DZQ on the signal. The cumulative performance calculated from the whole dataset based on respective $SNR_{IN}$ is depicted in Table 3 and Table 4. Lastly, the comparison among the existing methods of VCG signal compression and proposed technique is provided in Table 5. The visual and quantitative estimation derived from the proposed method facilitates the widening of the scope of research in the field of VCG compression and denoising.

**Table 1.** Quantitative analysis on the noisy VCG signals of the subjects for different given noise input SNRs.

| $SNR_{IN}$ | Subjects | MSE | PSNR | $SNR_{OUT}$ | $SNR_{IMP}$ | PRD |
|---|---|---|---|---|---|---|
| 10 dB | s0100lre | 0.00001619 | 43.428 | 28.315 | 18.315 | 3.852 |
| | s0200_re | 0.00014829 | 39.078 | 25.799 | 15.799 | 5.462 |
| | s0300lre | 0.00005712 | 43.240 | 27.307 | 17.307 | 4.333 |
| | s0400_re | 0.00024902 | 36.450 | 23.835 | 13.835 | 7.396 |
| | s0500_re | 0.00002377 | 41.978 | 28.172 | 18.172 | 3.915 |
| 5 dB | s0100lre | 0.00004115 | 39.482 | 24.369 | 19.369 | 6.063 |
| | s0200_re | 0.00037046 | 35.845 | 22.566 | 17.566 | 7.613 |
| | s0300lre | 0.00014084 | 39.735 | 23.803 | 18.803 | 6.538 |
| | s0400_re | 0.00070359 | 33.357 | 20.743 | 15.743 | 9.949 |
| | s0500_re | 0.00006462 | 38.023 | 24.217 | 19.217 | 6.236 |
| 0 dB | s0100lre | 0.00012111 | 34.853 | 19.740 | 19.740 | 10.340 |
| | s0200_re | 0.00107905 | 32.104 | 18.825 | 18.825 | 11.775 |
| | s0300lre | 0.00040415 | 35.425 | 19.492 | 19.492 | 10.827 |
| | s0400_re | 0.00213915 | 29.978 | 17.363 | 17.363 | 14.658 |
| | s0500_re | 0.00019344 | 33.466 | 19.659 | 19.659 | 10.617 |
| -5 dB | s0100lre | 0.00037391 | 29.985 | 14.872 | 19.872 | 18.120 |
| | s0200_re | 0.00332796 | 27.808 | 14.529 | 19.529 | 19.655 |
| | s0300lre | 0.00123499 | 30.692 | 14.760 | 19.760 | 18.748 |
| | s0400_re | 0.00667775 | 26.229 | 13.614 | 18.614 | 23.382 |
| | s0500_re | 0.00059925 | 28.639 | 14.833 | 19.833 | 18.570 |
| -10 dB | s0100lre | 0.00117473 | 25.024 | 9.911 | 19.911 | 32.083 |
| | s0200_re | 0.01045226 | 23.099 | 9.820 | 19.820 | 34.153 |
| | s0300lre | 0.00385885 | 25.793 | 9.860 | 19.860 | 33.015 |
| | s0400_re | 0.02102656 | 22.007 | 9.392 | 19.392 | 39.449 |
| | s0500_re | 0.00188105 | 23.695 | 9.888 | 19.888 | 32.844 |

**Table 2.** Quantitative analysis for compression on the VCG signals of the subjects for different given noise input SNRs.

| $SNR_{IN}$ | Subjects | CR | PRD | PSNR | SNR | MSE |
|---|---|---|---|---|---|---|
| 1 0 dB | s0100lre | 80.240 | 4.178 | 9.870 | 21.154 | 0.00006972 |
| | s0200_re | 59.525 | 3.542 | 11.093 | 29.506 | 0.00024277 |
| | s0300lre | 47.821 | 5.009 | 11.096 | 14.757 | 0.00007836 |
| | s0400_re | 92.045 | 3.647 | 10.685 | 27.853 | 0.00048688 |
| | s0500_re | 82.620 | 5.025 | 9.415 | 14.585 | 0.00012786 |
| 5 dB | s0100lre | 44.923 | 4.938 | 9.381 | 15.144 | 0.00009770 |
| | s0200_re | 70.727 | 3.463 | 11.155 | 30.857 | 0.00023265 |
| | s0300lre | 51.782 | 4.999 | 11.101 | 14.819 | 0.00007813 |
| | s0400_re | 70.068 | 3.476 | 10.833 | 30.654 | 0.00044726 |
| | s0500_re | 88.024 | 3.615 | 10.359 | 28.184 | 0.00006641 |
| 0 dB | s0100lre | 52.219 | 4.119 | 9.887 | 21.770 | 0.00006860 |
| | s0200_re | 93.208 | 3.645 | 10.997 | 27.857 | 0.00025931 |
| | s0300lre | 69.435 | 5.456 | 10.841 | 12.439 | 0.00009354 |
| | s0400_re | 91.266 | 3.710 | 10.649 | 26.913 | 0.00052648 |
| | s0500_re | 83.857 | 4.015 | 10.036 | 22.845 | 0.00008273 |
| -5 dB | s0100lre | 64.651 | 4.159 | 9.817 | 21.355 | 0.00007192 |
| | s0200_re | 91.123 | 3.712 | 10.918 | 26.857 | 0.00027396 |
| | s0300lre | 63.210 | 4.796 | 11.196 | 16.097 | 0.00007310 |

| | | | | | | |
|---|---|---|---|---|---|---|
| | s0400_re | 85.837 | 3.639 | 11.078 | 27.969 | 0.00055939 |
| | s0500_re | 86.665 | 5.177 | 9.247 | 13.745 | 0.00014153 |
| 10 dB | s0100lre | 95.990 | 4.492 | 10.441 | 18.310 | 0.00009114 |
| | s0200_re | 93.013 | 3.717 | 10.832 | 26.791 | 0.00029095 |

| | | | | | | |
|---|---|---|---|---|---|---|
| | s0300lre | 69.006 | 4.946 | 11.054 | 15.140 | 0.00008047 |
| | s0400_re | 118.290 | 3.898 | 12.193 | 24.374 | 0.00083365 |
| | s0500_re | 93.330 | 5.437 | 9.427 | 12.467 | 0.00017138 |

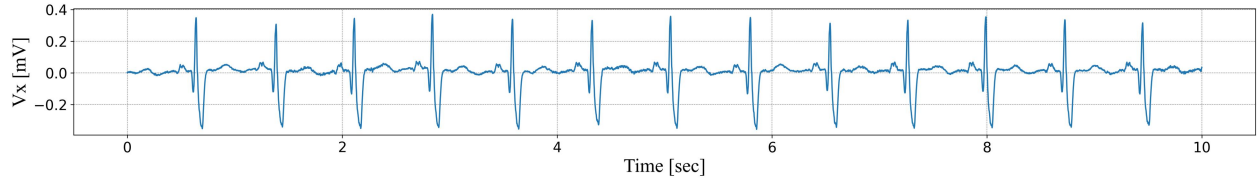


(a-i) $V_x$ component of the VCG signal

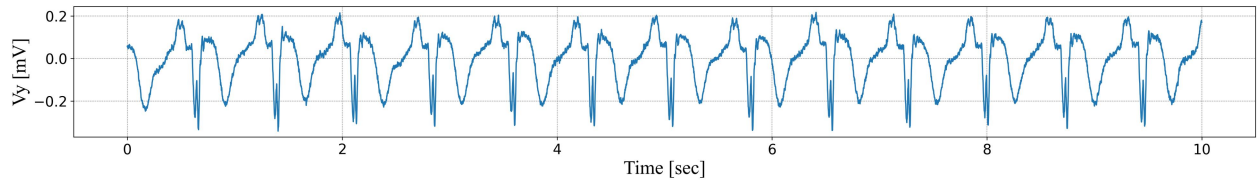


(a-ii) $V_y$ component of the VCG signal

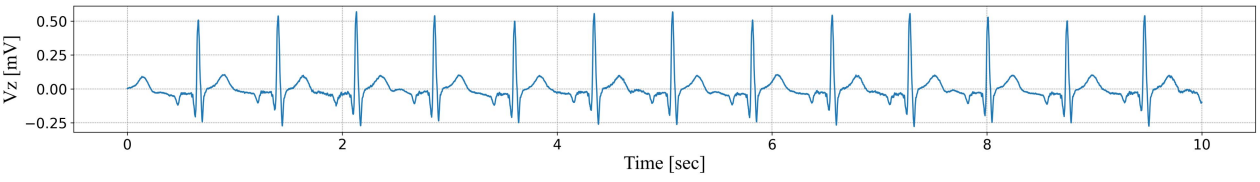


(a-iii) $V_z$ component of the VCG signal

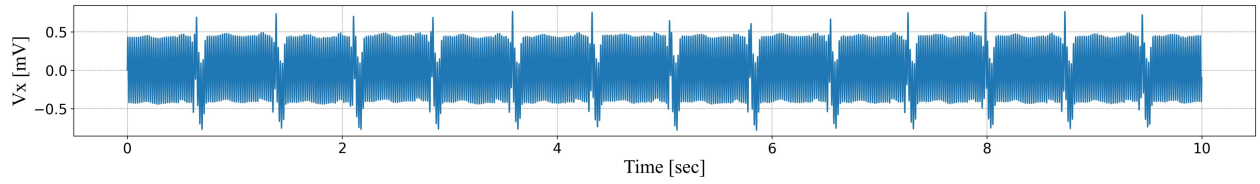


(b-i) Noise altered $V_x$ component of the VCG signal having input SNR set to -10 dB

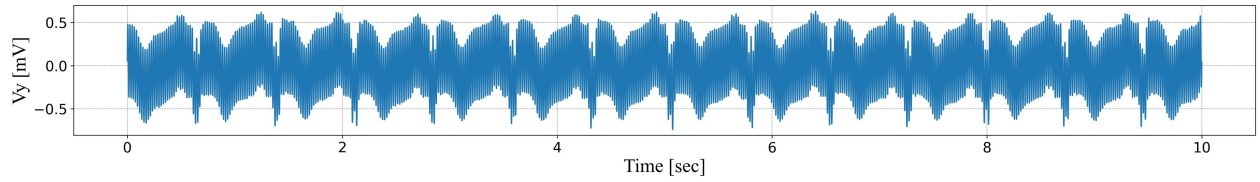


(b-ii) Noise altered $V_y$ component of the VCG signal having input SNR set to -10 dB

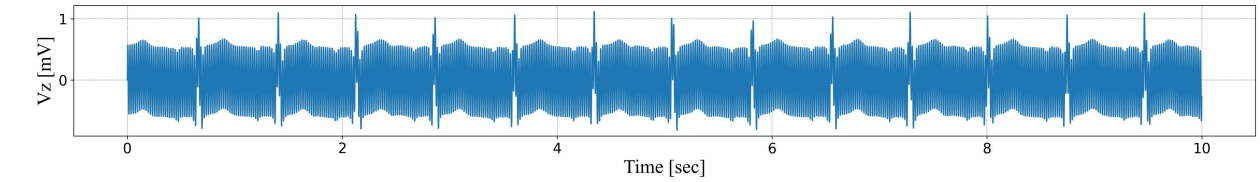


(b-iii) Noise altered $V_z$ component of the VCG signal having input SNR set to -10 dB

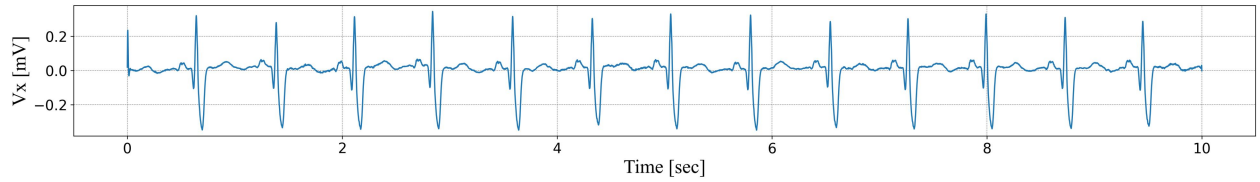


(c-i) Noise suppressed $V_x$ component of the VCG signal for input SNR set to -10 dB

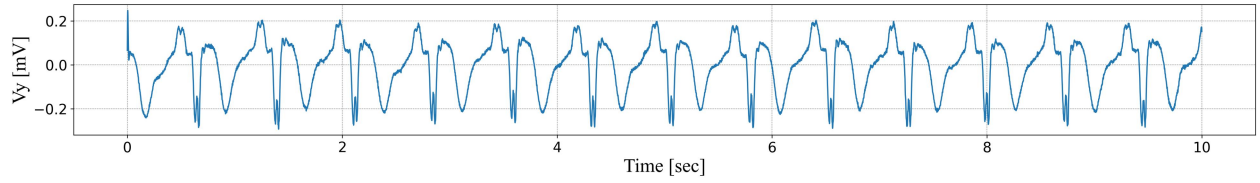


(c-ii) Noise suppressed $V_y$ component of the VCG signal for input SNR set to -10 dB

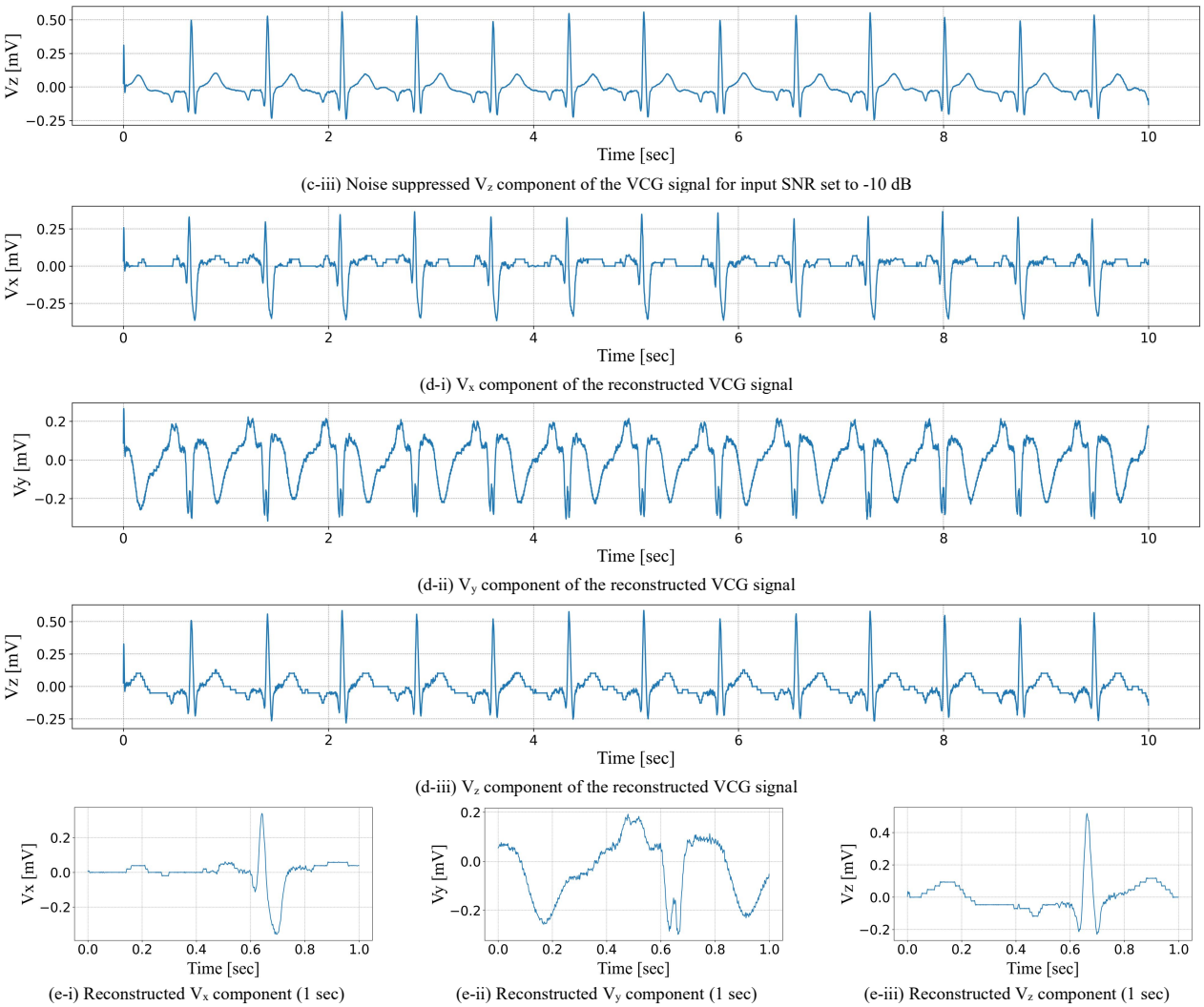


(c-iii) Noise suppressed $V_z$ component of the VCG signal for input SNR set to -10 dB

(d-i) $V_x$ component of the reconstructed VCG signal

(d-ii) $V_y$ component of the reconstructed VCG signal

(d-iii) $V_z$ component of the reconstructed VCG signal

(e-i) Reconstructed $V_x$ component (1 sec)

(e-ii) Reconstructed $V_y$ component (1 sec)

(e-iii) Reconstructed $V_z$ component (1 sec)

**Fig. 4.** Graphical representation of various outcomes involved in the denoising and compression process of the algorithm.

**Table 3.** Cumulative denoising performance metric results as obtained from the whole dataset.

| $SNR_{INPUT}$ | MSE | PSNR | $SNR_{OUT}$ | $SNR_{IMP}$ | PRD |
|---|---|---|---|---|---|
| 10 | 0.000111 | 40.85885 | 26.61351 | 16.61351 | 5.127953 |
| 5 | 0.000274 | 37.46932 | 23.22398 | 18.22398 | 7.370022 |
| 0 | 0.000791 | 33.37318 | 19.12784 | 19.12784 | 11.72686 |
| -5 | 0.002424 | 28.82343 | 14.57809 | 19.57809 | 19.83917 |
| -10 | 0.007592 | 24.02752 | 9.782179 | 19.78218 | 34.57598 |

**Table 4.** Cumulative compression performance metric results as obtained from the whole dataset.

| $SNR_{INPUT}$ | CR | PRD | PSNR | SNR | MSE |
|---|---|---|---|---|---|
| 10 | 71.38043 | 4.446720 | 10.41856 | 19.96106 | 0.000200 |
| 5 | 74.68949 | 4.443744 | 10.43369 | 19.98779 | 0.000190 |
| 0 | 78.30261 | 4.436309 | 10.47152 | 19.95447 | 0.000195 |
| -5 | 80.82911 | 4.470615 | 10.53784 | 19.56182 | 0.000221 |
| -10 | 86.07420 | 4.545420 | 10.72010 | 18.81231 | 0.000258 |

The comparative study highlighted in Table 5 demonstrates the effectiveness of the proposed method in achieving a favourable balance between compression efficiency and reconstruction quality when compared with existing VCG signal compression approaches. This comparison is drawn by the use of some important parameters such as; *CR, PRD, SNR, QS,* and *MSE*.

**Table 5.** Comparative study of numerous VCG compression approaches.

| S.NO | Method | CR | PRD | SNR | QS | MSE |
|---|---|---|---|---|---|---|
| 1. | DCT with NNI [36] | 35.04 | 2.45 | 35.62 | 15.69 | - |
| 2. | KLT+TQWT [22] | 15.43 | 7.39 | - | 2.13 | - |
| 3. | SVD [37] | 6.55 | 4.90 | 28.09 | - | $2.61*10^{-4}$ |
| 4. | 2D DCT [38] | 5.00 | - | - | - | - |
| 5. | 2D WHT [38] | 2.00 | - | - | - | - |
| 6. | KLT [11] | 12.00 | - | - | - | - |
| 7. | HE [39] | 3.02 | 16.90 | - | - | - |

| | | | | | | |
|---|---|---|---|---|---|---|
| 8. | HE+DCT [39] | 4.15 | 17.20 | - | - | - |
| 9. | DWT+SVSR [40] | 9.91 | 2.10 | - | - | $1.67*10^{-3}$ |
| **10.** | **Proposed** | **71.38** | **4.44** | **19.96** | **16.05** | **$2.00*10^{-4}$** |

From Table 5 it is observed that the proposed method significantly outperforms all compared techniques. When comparing in terms of *CR*, proposed approach achieves improvements of 50.9% over DCT with NNI, 78.4% over KLT+TQWT, 90.8% over SVD, 93.0% over 2D DCT, 97.2% over 2D WHT, 83.2% over KLT, 95.8% over HE, 94.2% over HE+DCT, and 86.1% over DWT+SVSR. With respect to reconstruction distortion, the proposed method exhibits lower *PRD* than KLT+TQWT, HE, and HE+DCT, while remaining comparable to SVD; however, it is inferior to DCT with NNI and DWT+SVSR, which achieve lower *PRD* at substantially lower compression ratios. In terms of *SNR*, although DCT with NNI and SVD report higher values due to conservative compression, the proposed method maintains acceptable *SNR* under significantly higher compression levels. The proposed approach achieves the highest quality score, improving *QS* by 2.2% over DCT with NNI and 86.7% over KLT+TQWT, confirming its superior compression–quality balance. Furthermore, the proposed method yields lower *MSE* than DWT+SVSR and comparable performance to SVD, despite operating at much higher compression ratios. Overall, while some existing techniques excel in isolated performance metrics, the proposed method consistently delivers superior compression efficiency with controlled distortion, making it a more effective approach for VCG signal compression.

## 4 Conclusion

The VCG denoising and compression technique proposed here adheres to the powerline noise suppression and amalgamation of different techniques for compression of the signal. The involvement of VMD and notch filter enhances the denoising performance followed by the mode-wise implementation of TQWT on EMD's IMFs to produce coefficient matrix for the deployment of deadzone quantization and RLE for compressing the signal. The quantitative and qualitative analysis of the algorithm obtained from utilization of the performance matrix solidifies the proposition discussed in the work to consolidate the performance of the proposed method to suppress the noise and have the characteristics of a compressed signal. This method achieves an average *MSE* value in the order of 10-5, a good *PSNR*, $SNR_{OUT}$, and $SNR_{IMP}$ value, with a lower *PRD*, when inquired about the denoising performance. It yields a greater *CR*, *SNR* scores, associated with a lesser *MSE* and *PRD* score, with respect to compressing the signal. The superiority of the algorithm is verified and validated over the whole dataset to conclude that this algorithm sets a benchmark for further enhancement in the field of VCG signal processing.

***Corresponding author:** Aditya Tiwari, email : adityatanu7@gmail.com

**Declarations**

***Funding Details:*** This work is supported by the Science and Engineering Research Board (SERB) under Grant No. EEQ/2023/000061.

***Conflict of Interest:*** There is no conflict of interest among the authors.

***Availability of Data and Material:*** The dataset analysed during the current study is publicly available on PhysioNet as the PTB Diagnostic ECG Database, accessible at: https://doi.org/10.13026/C28C71.

***Code Availability***: The custom MATLAB codes used in this study are available from the corresponding author upon reasonable request.

***Ethical Statement:*** This research did not involve any human or animals participants.

***Consent to Participate:*** Not applicable.

***Consent for Publication:*** All authors consent to publication of this manuscript.

**ORCID:** The ORCID ID's of the authors are as follows:

H. Gupta : https://orcid.org/0000-0002-0187-0433.

Aditya Tiwari: https://orcid.org/0009-0000-1863-7171.

A. Kumar: https://orcid.org/0000-0002-3945-4646.

## References

[1] U.S National Cancer Institute, Body Functions & Life Process - SEER Training, 2019 (n.d.).

[2] S.S. Barold, Willem Einthoven and the birth of clinical electrocardiography a hundred years ago, Card. Electrophysiol. Rev. 7 (2003) 99–104.

[3] P. Gloor, Hans Berger on Electroencephalography, Am. J. EEG Technol. 9 (1969) 1–8.

[4] G.E. Burch, The history of vectorcardiography, Med. Hist. 29 (1985) 103–131.

[5] C.L. Levkov, Orthogonal electrocardiogram derived from the limb and chest electrodes of the conventional 12-lead system, Med. Biol. Eng. Comput. 25 (1987) 155–164.

[6] J. Huang, C. Wang, W. Zhao, A. Grau, X. Xue, F. Zhang, LTDNet-EEG: A Lightweight Network of Portable/Wearable Devices for Real-Time EEG Signal Denoising, IEEE Trans. Consum. Electron. (2024).

[7] M. Geng, X. Meng, J. Yu, L. Zhu, L. Jin, Z. Jiang, B. Qiu, H. Li, H. Kong, J. Yuan, K. Yang, H. Shan, H. Han, Z. Yang, Q. Ren, Y. Lu, Content-Noise Complementary Learning for Medical Image Denoising, IEEE Trans. Med. Imaging 41 (2022) 407–419.

[8] Q. Sun, J. Li, C. Liang, R. Liu, J. Pang, Y. Chen, C. Wang, Multiscale Joint Recurrence Quantification Analysis Integrating ECG Spatiotemporal and Dynamic Information for Cardiopathy Detection, IEEE Trans. Instrum. Meas. 73 (2024) 1–13.

[9] T.M. Chen, Y.H. Tsai, H.H. Tseng, K.C. Liu, J.Y. Chen, C.H. Huang, G.Y. Li, C.Y. Shen, Y. Tsao, SRECG: ECG Signal Super-Resolution Framework for Portable/Wearable Devices in Cardiac Arrhythmias Classification, IEEE Trans. Consum. Electron. 69 (2023) 250–260.

[10] B. Jiang, Y. Lu, X. Chen, X. Lu, G. Lu, Graph Attention in Attention Network for Image Denoising, IEEE Trans. Syst. Man, Cybern. Syst. 53 (2023) 7077–7088.

[11] M.E. Womble, J.S. Halliday, S.K. Mitter, M.C. Lancaster, J.H. Triebwasser, Data Compression for Storing and Transmitting ECG's/VCG's, Proc. IEEE 65 (1977) 702–706.

[12] S. Banerjee, G.K. Singh, Quality Guaranteed ECG Signal Compression Using Tunable-Q Wavelet Transform and Möbius Transform-Based AFD, IEEE Trans. Instrum. Meas. 70 (2021) 1–11.

[13] K. Hayashi, R. Kohno, N. Akamatsu, D.G. Benditt, H. Abe, Abnormal repolarization: A common electrocardiographic finding in patients with epilepsy, J. Cardiovasc. Electrophysiol. 30 (2019) 109–115.

[14] G.D. Clifford, ECG Statistics, Noise, Artifacts, and Missing Data, (n.d.).

[15] J.A. Van Alsté, T.S. Schilder, Removal of Base-Line Wander and Power-Line Interference from the ECG by an Efficient FIR Filter with a Reduced Number of Taps, IEEE Trans. Biomed. Eng. BME-32 (1985) 1052–1060.

[16] L. Frølich, I. Dowding, Removal of muscular artifacts in EEG signals: a comparison of linear decomposition methods, Brain Informatics 5 (2018) 13–22.

[17] S. Chatterjee, R.S. Thakur, R.N. Yadav, L. Gupta, D.K. Raghuvanshi, Review of noise removal techniques in ECG signals, IET Signal Process. 14 (2020) 569–590.

[18] S. Jain, V. Bajaj, A. Kumar, Effective de-noising of ECG by optimised adaptive thresholding on noisy modes, IET Sci. Meas. Technol. 12 (2018) 640–644.

[19] H.Y. Mir, O. Singh, Powerline interference reduction in ECG signals using variable notch filter designed via variational mode decomposition, Analog Integr. Circuits Signal Process. 118 (2024) 317–328.

[20] B.H. Tracey, E.L. Miller, Nonlocal means denoising of ECG signals, IEEE Trans. Biomed. Eng. 59 (2012) 2383–

2386.

[21] R.N. Vargas, A.C.P. Veiga, Electrocardiogram signal denoising by a new noise variation estimate, Res. Biomed. Eng. 36 (2020) 13–20.

[22] R. Vimal, A. Kumar, A. Tiwari, A new VCG signal compression technique based on discrete Karhunen-Loeve expansion and tunable quality wavelet transform, J. Electrocardiol. 89 (2025) 153894.

[23] S.M.S. Jalaleddine, C.G. Hutchens, R.D. Strattan, W.A. Coberly, ECG Data Compression Techniques—A Unified Approach, IEEE Trans. Biomed. Eng. 37 (1990) 329–343.

[24] A.A. Shinde, P. Kanjalkar, The comparison of different transform based methods for ECG data compression, in: 2011 - Int. Conf. Signal Process. Commun. Comput. Netw. Technol. ICSCCN-2011, 2011: pp. 332–335.

[25] A.M. Kamal, T. Sakorikar, U.M. Pal, H.J. Pandya, Engineering Approaches for Breast Cancer Diagnosis: A Review, IEEE Rev. Biomed. Eng. 16 (2023) 687–705.

[26] W.C. Mueller, Arrhythmia detection program for an ambulatory ECG monitor, Biomed. Sci. Instrum. 14 (1978) 81–85.

[27] C.K. Jha, M.H. Kolekar, Empirical Mode Decomposition and Wavelet Transform Based ECG Data Compression Scheme, IRBM 42 (2021) 65–72.

[28] K. Akazawa, T. Uchiyama, S. Tanaka, A. Sasamori, E. Harasawa, Adaptive data compression of ambulatory ECG using multi templates, in: Comput. Cardiol., Publ by IEEE, 1993: pp. 495–498.

[29] S.J. Simske, D.R. Blakley, Using the vectorcardiogram to remove ECG noise, in: Proc. - Int. Conf. Image Process. ICIP, 2012: pp. 2301–2304.

[30] Nutzung der EKG-Signaldatenbank CARDIODAT der PTB über das Internet, Biomed. Tech. / Biomed. Eng. 40 (n.d.) 317–318.

[31] W. Xu, A. Li, B. Shi, J. Zhao, A Novel Design of Sparse FIR Multiple Notch Filters with Tunable Notch Frequencies, Math. Probl. Eng. 2018 (2018).

[32] K. Dragomiretskiy, D. Zosso, Variational Mode Decomposition, IEEE Trans. Signal Process. 62 (2014) 531–544.

[33] I.W. Selesnick, Wavelet transform with tunable Q-factor, IEEE Trans. Signal Process. 59 (2011) 3560–3575.

[34] C.K. Jha, M.H. Kolekar, Tunable Q-wavelet based ECG data compression with validation using cardiac arrhythmia patterns, Biomed. Signal Process. Control 66 (2021) 102464.

[35] S. Akhter, M.A. Haque, ECG comptression using run length encoding, in: 2010 18th Eur. Signal Process. Conf., 2010: pp. 1645–1649.

[36] A. Tiwari, R. Vimal, A. Kumar, Compression and Reconstruction of VCG Signal Based on DCT and Nearest Neighbour Interpolation, in: 2024 IEEE 8th Int. Conf. Inf. Commun. Technol., 2024: pp. 1–6.

[37] D. Mishra, A. Kumar, VCG signal compression based on singular value decomposition, Int. J. Electron. Lett. 13 (2025) 280–290.

[38] S.A. Dyer, N. Ahmed, D.R. Hummels, Vectorcardiographic Data Compression via Walsh And Cosine Transforms, IEEE Trans. Electromagn. Compat. EMC-27 (1985) 24–34.

[39] P. Augustyniak, The Use of Predictive Coding for Effective Compression of Vectocardiograms, IFMBE Vol.1 (2001) 364–367.

[40] D. Mishra, A. Kumar, Vectorcardiogram signal compression: A hybrid approach using discrete wavelet transform and singular vector sparse reconstruction, J. Electrocardiol. 91 (2025) 154042.